

Synthesis and isolation of two high-nuclearity manganese(II) imido compounds: structural characterization of a compound containing a $[\text{Mn}_6(\mu_3\text{-NPh})_4]^{4+}$ core†

Warren J. Grigsby and Philip P. Power*

Department of Chemistry, University of California, Davis, CA 95616, USA

The reaction of the imide transfer agent $[\{\text{Mg}(\text{NPh})(\text{thf})\}_6]$ (thf = tetrahydrofuran) with MnBr_2 led to the isolation of the polynuclear manganese(II) imido compounds $[\{\text{Mn}_6(\mu_3\text{-NPh})_4\text{Br}_3(\text{thf})_4\}\{\text{Mg}_2(\mu\text{-NHPH})(\mu\text{-Br})_2\text{Br}_2(\text{thf})_4\}]\cdot 3\text{C}_6\text{H}_5\text{Me}$ and $[\text{Mn}_6(\mu_3\text{-NPh})_4\text{Br}_4(\text{thf})_6]$ in moderate yield. A crystal structure analysis of the former revealed a formally cationic, adamantane-like Mn_6N_4 structure linked to a dimagnesium centred counter anion *via* Br^- bridges.

There is widespread interest in the synthesis and magnetic properties of high-nuclearity manganese compounds owing, primarily, to their relevance to biological systems particularly the manganese centres in photosystem II.¹ The majority of these compounds contain either carboxylato or oxo ligands which form bridges between the metal centres.² Imido ligands, which are isoelectronic or isolobal to the oxide ion, have not been used to stabilize such polynuclear compounds. Nonetheless, the syntheses of a number of highly interesting mono-, bi- and tri-nuclear imido derivatives of manganese have been reported.³ These compounds, however, concern manganese in the higher oxidation states v–vii. Recent work has shown that the magnesium imide compound $[\{\text{Mg}(\text{NPh})(\text{thf})\}_6]$ **1** (thf = tetrahydrofuran) is an effective NPh^{2-} transfer agent for a number of substrates.⁴ Noting the similar sizes of the Mg^{2+} and Mn^{2+} ions⁵ it was decided to test the reactions of **1** with MnBr_2 . The products $[\{\text{Mn}_6(\mu_3\text{-NPh})_4\text{Br}_3(\text{thf})_4\}\{\text{Mg}_2(\mu\text{-NHPH})(\mu\text{-Br})_2\text{Br}_2(\text{thf})_4\}]\cdot 3\text{C}_6\text{H}_5\text{Me}$ **2** and $[\text{Mn}_6(\mu_3\text{-NPh})_4\text{Br}_4(\text{thf})_6]$ **3** are now described.

Experimental

General techniques and reagents

All reactions were performed by using modified Schlenk techniques under an inert atmosphere of N_2 or in a Vacuum Atmospheres HE43-2 dry-box. Solvents were freshly distilled under N_2 from Na/K or sodium–potassium–benzophenone and degassed twice prior to use. Proton NMR spectra were obtained on a General Electric QE-300 NMR spectrometer and referenced to an internal standard, IR spectra as Nujol mulls between CsI plates employing a Perkin-Elmer 1430 spectrometer, and EPR spectra using a Bruker 200D spectrometer. Compound **1** was prepared by the literature method⁴ and MnBr_2 was obtained commercially and used as received.

Syntheses

$[\{\text{Mn}_6(\mu_3\text{-NPh})_4\text{Br}_3(\text{thf})_4\}\{\text{Mg}_2(\mu\text{-NHPH})(\mu\text{-Br})_2\text{Br}_2(\text{thf})_4\}]\cdot 3\text{C}_6\text{H}_5\text{Me}$ **2**. Manganese dibromide (0.86 g, 4.0 mmol) was dissolved in thf (40 cm^3) and compound **1** (0.75 g, 0.67 mmol) was added *via* a solids-addition funnel. The solution was heated to *ca.* 50 °C for 16 h. All the volatile materials were removed under reduced pressure and the resulting red residue was extracted with toluene (50 cm^3). The deep red solution was filtered through a frit and concentrated to incipient

crystallization. Cooling slowly in a –20 °C freezer yielded red prisms of **2** (0.97 g, 0.43 mmol, 65% based on manganese). Loss of solvent at 170 °C, melting at 253 °C. ¹H NMR (C_6D_6): δ 3.1–2.9 (s, br). IR: 1575ms, 1210s, 1175ms, 1070w, 1025s, 990m (sh), 910w, 865ms, 835m, 815ms, 775w, 750ms, 725m, 685m, 620m, 570s, 505m, 435s, 340w and 270ms cm^{-1} . $\mu_{\text{eff}} = 3.37 \mu_{\text{B}}$ at 298 K.

$[\text{Mn}_6(\mu_3\text{-NPh})_4\text{Br}_4(\text{thf})_6]$ **3**. Manganese dibromide (0.86 g, 4.0 mmol) was dissolved in thf (20 cm^3) and compound **1** (0.75 g, 0.67 mmol) was added *via* a solids-addition funnel. Then, 1,4-dioxane (1 cm^3 , 12 mmol) was added *via* a syringe and the solution was refluxed for 16 h. All volatile materials were removed under reduced pressure and the resulting residue extracted with toluene (40 cm^3). The solution was filtered through a frit and then concentrated to *ca.* 10 cm^3 . After layering with hexane (10 cm^3) the solution was cooled to –20 °C to give a fine pink powder. This was redissolved with the minimum amount of thf and layered with hexane (2 cm^3). Slow cooling to –20 °C yielded fine red needles of **3** (0.30 g, 0.21 mmol, 31% based on Mn). Darkens at 230 °C but does not melt < 325 °C. ¹H NMR (C_6D_6): δ 3.3 (s, br). IR: 1600mw, 1575m, 1260m, 1150w, 1070m, 1020s, 920w, 865mw, 800m, 770mw, 750mw, 920w, 685s (sh), 620w, 650m (br), 450w, 275m and 240mw cm^{-1} (Found: C, 39.5; H, 5.0; N, 3.3. $\text{C}_{48}\text{H}_{68}\text{Br}_4\text{Mn}_6\text{N}_4\text{O}$: C, 39.85; H, 4.75; N, 3.85%). $\mu_{\text{eff}} = 3.33 \mu_{\text{B}}$ at 298 K. Unit-cell lattice parameters at 130 K: $a = 21.796(9)$, $b = 12.647(5)$, $c = 22.088(9)$ Å, $\alpha = \beta = \gamma = 90^\circ$, $U = 6088(4)$ Å³.

X-Ray crystallography

Crystal data for compound 2. 130 K, Mo-K α ($\lambda = 0.71073$ Å) radiation, $\text{C}_{83}\text{H}_{114}\text{Br}_7\text{Mg}_2\text{Mn}_6\text{N}_5\text{O}_8$, $M = 2247.4$, crystal dimensions 0.58 × 0.40 × 0.12 mm, $a = 13.159(3)$, $b = 18.163(4)$, $c = 20.978(4)$ Å, $\alpha = 101.52(3)$, $\beta = 94.20(3)$, $\gamma = 108.50(3)^\circ$, $U = 4608(2)$ Å³, $Z = 2$, space group $P\bar{1}$, $\mu = 3.899$ mm^{-1} , $D_c = 1.619$ Mg m^{-3} , 2 θ range 0–45°.

A crystal of compound **2** suitable for X-ray data collection was selected and mounted in the cold stream (130 K) of a Siemens R3m/v diffractometer equipped with a LT-1 low-temperature device. Data were collected in a triclinic cell setting. The structure was solved in space group $P\bar{1}$ using direct and Fourier-difference methods.⁶ It was developed and refined routinely.⁶ Two thf molecules exhibited disorder which was satisfactorily modelled using split occupancies. The disordered atoms C(49) and C(58) were disordered into two positions A and B; C(49A) and C(49B) converged with occupancies of 53

† Non-SI Unit employed: $\mu_{\text{B}} \approx 9.27 \times 10^{-24}$ J T⁻¹.

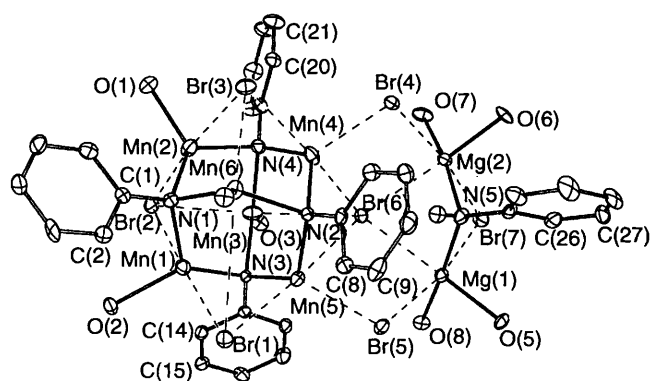


Fig. 1 Thermal ellipsoidal plot (30% probability) of compound 2. Hydrogen atoms [except H(1)] and the carbon atoms of the thf molecules have been omitted for clarity

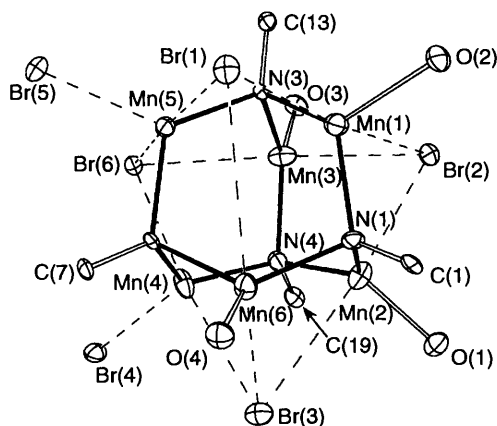


Fig. 2 Thermal ellipsoidal plot (30% probability) of the cationic $\text{Mn}_6(\text{NPh})_4$ core of compound 2. For clarity, only *ipso*-carbon atoms of the phenyl rings and oxygen atoms of the thf molecules are shown

Table 1 Selected bond lengths (Å) and angles (°) for $[\{\text{Mn}_6(\mu_3\text{-NPh})_4\text{Br}_3(\text{thf})_4\}\{\text{Mg}_2(\mu\text{-NHPH})(\mu\text{-Br})_2\text{Br}_2(\text{thf})_4\}]\cdot 3\text{C}_6\text{H}_5\text{Me } 2$

Br(4)–Mn(4)	2.545(2)	Mn(3)–N(4)	2.047(8)
Br(4)–Mg(2)	2.693(4)	Mn(3)–N(3)	2.053(8)
Br(5)–Mn(5)	2.552(2)	Mn(4)–N(4)	2.034(9)
Br(5)–Mg(1)	2.728(4)	Mn(4)–N(2)	2.079(8)
Br(6)–Mg(2)	2.819(4)	Mn(5)–N(3)	2.044(8)
Br(6)–Mg(1)	2.823(4)	Mn(5)–N(2)	2.048(8)
Br(7)–Mg(2)	2.680(4)	Mn(6)–N(1)	2.035(9)
Br(7)–Mg(1)	2.782(4)	Mn(6)–N(2)	2.065(8)
Mn(1)–N(1)	2.052(8)	Mn–O	2.133(7)*
Mn(1)–N(3)	2.066(8)	Mg–O	2.070(8)*
Mn(2)–N(4)	2.064(9)	Mg–N	2.116(9)*
Mn(2)–N(1)	2.080(9)		
Mn(4)–Br(4)–Mg(2)	100.86(9)	N(4)–Mn(3)–O(3)	124.0(3)
Mn(5)–Br(5)–Mg(1)	110.13(9)	N(3)–Mn(3)–O(3)	115.1(3)
Mg(2)–Br(6)–Mg(1)	68.86(10)	N(4)–Mn(4)–N(2)	121.7(3)
Mg(2)–Br(7)–Mg(1)	71.45(11)	N(4)–Mn(4)–Br(4)	120.7(3)
N(1)–Mn(1)–N(3)	120.8(3)	N(2)–Mn(4)–Br(4)	117.4(2)
N(1)–Mn(1)–O(2)	108.3(3)	N(3)–Mn(5)–N(2)	124.9(2)
N(3)–Mn(1)–O(2)	127.9(3)	N(2)–Mn(5)–Br(5)	108.5(2)
N(4)–Mn(2)–N(1)	121.2(3)	N(1)–Mn(6)–N(2)	120.2(3)
N(4)–Mn(2)–O(1)	109.7(3)	N(1)–Mn(6)–O(4)	117.2(3)
N(1)–Mn(2)–O(1)	127.8(3)	N(2)–Mn(6)–O(4)	113.9(3)
N(4)–Mn(3)–N(3)	120.6(3)		

* Average.

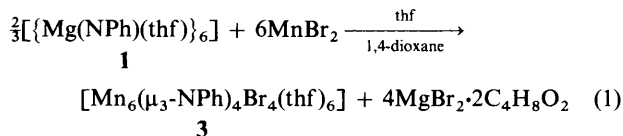
and 47% respectively and C(58A) and C(58B) with 43 and 57% respectively. All hydrogen atoms were added in calculated positions and refined using a riding model except for the N(5) hydrogen which was located on a difference map. For

practicality, the rings of the included toluene solvent molecules were constrained as rigid hexagons. An absorption correction (XABS 2) was applied.⁷ Refinement was by full-matrix least-squares methods, based on F^2 , with anisotropic thermal parameters for all non-hydrogen atoms not affected by disorder. Refinement converged with a residual R value = 0.062 for 7584 [$I > 2\sigma(I)$] data. The final difference map showed the greatest peak (0.77 e Å⁻³) adjacent to Br(5). Important structural data are given in Table 1.

Atomic coordinates, thermal parameters, and bond lengths and angles have been deposited at the Cambridge Crystallographic Data Centre (CCDC). See Instructions for Authors, *J. Chem. Soc., Dalton Trans.*, 1996, Issue 1. Any request to the CCDC for this material should quote the full literature citation and the reference number 186/246.

Results and Discussion

The reaction between the imide transfer agent $[\{\text{Mg}(\text{NPh})(\text{thf})_6\}]$ **1** and 6 equivalents of MnBr_2 in a thf solution led to the isolation of the unusual polynuclear compound $[\{\text{Mn}_6(\mu_3\text{-NPh})_4\text{Br}_3(\text{thf})_4\}\{\text{Mg}_2(\mu\text{-NHPH})(\mu\text{-Br})_2\text{Br}_2(\text{thf})_4\}]\cdot 3\text{C}_6\text{H}_5\text{Me } 2$ in moderate yield. Compound **2** is a rare example of a high-nuclearity manganese species, with a three-dimensional array of metal ions, in which the ligands do not bind through oxygen-based ligands. Furthermore, it appears to be a rare instance of a structurally characterized multinuclear transition-metal imide cage/cluster that is stable in the absence of ligands such as CO or $\eta^5\text{-C}_5\text{H}_5$.⁸ Repetition of the reaction between **1** and MnBr_2 in refluxing thf solution, in the presence of 1,4-dioxane, led to the isolation of $[\text{Mn}_6(\mu_3\text{-NPh})_4\text{Br}_4(\text{thf})_6]$ **3**, equation (1). Although both **2** and **3** are extremely air- and



moisture-sensitive compounds they possess high thermal stability. This is illustrated by the fact that compound **2** melts at 253 °C and **3** does not melt below 325 °C.

The geometry of compound **2** is shown in Fig. 1. The structure consists of a contact ion pair which can be regarded as consisting of a cationic moiety $[\text{Mn}_6(\mu_3\text{-NPh})_4\text{Br}_3(\text{thf})_4]^+$ (Fig. 2) which possesses an adamantane-like cage of manganese and nitrogen atoms. This $\text{Mn}_6(\mu_3\text{-NPh})_4$ adamantyl cage has μ_3 -phenylimido groups in the bridgehead positions and five-coordinate manganese ions in each of the six doubly bridging positions. The cage structure is broadly similar to the corresponding Mg_6N_4 array in $[\text{Mg}_6(\mu_3\text{-NPh})_4\text{Br}_4(\text{thf})_6]$.⁹ Four of the six Mn^{2+} ions are also solvated by thf donors. In addition three Br^- ions [*i.e.* Br(1), Br(2) and Br(3)] cap three of the Mn_3N_3 hexagonal faces of the Mn_6N_4 cage which involves four of the six Mn^{2+} ions in bonding to these Br^- ions. The Br^- ions, however, are asymmetrically μ_3 -bridging and exhibit significant variation in the Mn–Br distance (2.62–3.78 Å). The remaining two Mn^{2+} ions in the adamantyl Mn_6N_4 core are each bound to bromide ions which also bridge to Mg^{2+} centres in the counter ion. The latter may be described as a dinuclear dimagnesium species having a phenylamide group and two Br^- ions [Br(6) and Br(7)] bridging two Mg^{2+} centres. The Mg^{2+} ions are further bound to two Br^- ions [Br(4) and Br(5)] that also bridge to the Mn^{2+} centres. In addition, one of the Br^- ions [Br(6)] which bridges the two Mg^{2+} ions interacts with three Mn^{2+} ions [Mn(3), Mn(4), Mn(5)]. Thus the contact ion pairs are linked by three bridging Br^- ions Br(4), Br(5) and Br(6). The bridging Mn–Br distances for Br(4) and Br(5) are 2.545(2) and 2.552(2) Å, respectively. The weaker bridging interaction through Br(6) to Mn(3) (3.04 Å), Mn(4) (3.06 Å) and Mn(5) (3.47 Å) is reflected in the longer Mn–Br distances.

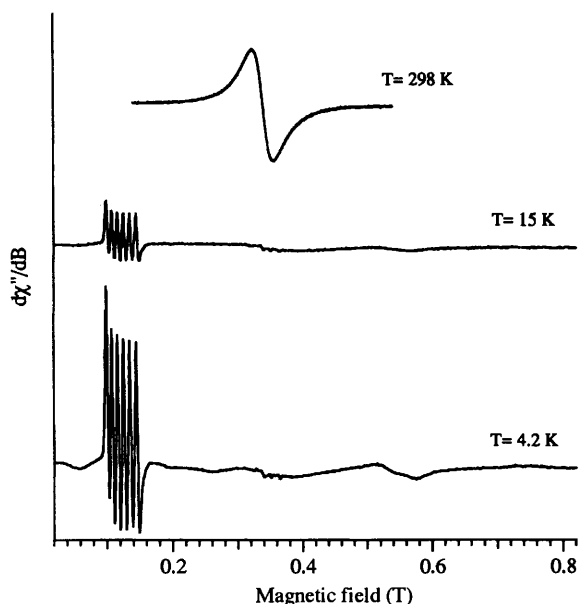


Fig. 3 Continuous-wave EPR spectra for compound **3** at 298, 15 and 4.2 K. For 4.2 K spectrum: $\nu = 9.55$ GHz, power = 0.050 mW, modulation amplitude = 12.5 G, modulation frequency = 100 kHz, sweep time = 100 s, time constant = 100.0 ms

The Mn–N distances (average 2.055 Å) in the Mn_6N_4 cage are longer than those observed in other manganese imido complexes in which nitrogen is bridging, for example $[\{\text{Mn}(\text{NBu}^t)_2(\mu\text{-NBu}^t)_2\}_2\text{Mn}]_3$ and $[\text{Mn}_2\text{R}_2(\text{NBu}^t)_2(\mu\text{-NBu}^t)_2]$.^{3c,d} However in these complexes the oxidation states of manganese are higher (v and vi) so that the smaller effective ionic radii⁵ of Mn^{5+} and Mn^{6+} result in shorter Mn–N bond lengths. There are also short Mn...Mn interactions (3.04–3.21 Å) in **2** and these distances are similar to those found for the manganese nitrogen heterocubane species $[\{\text{MnI}(\text{NPEt}_3)\}_4]$.¹⁰

The Mg–O [average 2.070(8) Å] and Mg–N (amido) distances [average 2.116(9) Å] of the anionic moiety are similar to those reported in a variety of complexes.¹¹ The Mg–Br distances are well within the known range,¹¹ although there exists some variation in these distances that can be rationalized on the basis of co-ordination number. The Mg–Br distances at which the Br^- ions link the cation and anion [Mg(1)–Br(5) 2.73 and Mg(2)–Br(4) 2.69 Å] are similar to those of the bridging Br^- ion, Br(7) (2.68 and 2.78 Å). The Mg–Br distances for the remaining Br^- are longer (average 2.82 Å) presumably due to the μ_3 co-ordination of Br(6) to the Mn^{2+} centres.

Although the crystal quality of compound **3** prevented an X-ray structural determination, the cell constants are nevertheless very close to those of the magnesium analogue $[\text{Mg}_6(\text{NPh})_4\text{Br}_4(\text{thf})_6]$ ⁹ which crystallized from a 'PhN(MgBr)₂' solution formed by the addition of 2 equivalents of a Grignard reagent to H_2NPh .¹² This result is not entirely unexpected given the similar ionic sizes of manganese and magnesium.⁵ The similarity of the cell constants for **3** and its magnesium analogue as well as the existence of the Mn_6N_4 adamantyl structural motif in **2** suggest that the structure of **3** is very similar to that of $[\text{Mg}_6(\text{NPh})_4\text{Br}_4(\text{thf})_6]$.⁹

Both compounds **2** and **3** give paramagnetically shifted ¹H NMR spectra. The X-band EPR spectra (in toluene) at room temperature both show a broad structureless feature at $g =$

1.994(1). Upon cooling to 4.2 K the spectrum for **3** resolves into a six-line pattern at $g = 5.761(1)$ which results from anisotropy (Fig. 3). The ⁵⁵Mn hyperfine splitting at this field (A_{\parallel}) is 0.0091(8) T. The parallel turning point is not clearly observed, and may be broadened by g strain. When cooled to 4.2 K weak features are observed at $g = 1.18$ and ≈ 2.0 . These EPR signals are likely due to high-spin Mn^{2+} ($S = \frac{5}{2}$) with zero-field splitting interactions (D) larger than the microwave frequency.¹³

Measurement of the magnetic susceptibility of compound **2** at 298 K gave a magnetic moment of $\mu_{\text{eff}} = 3.4 \mu_{\text{B}}$ per manganese atom. For **3** a similar magnetic moment of $\mu_{\text{eff}} = 3.3 \mu_{\text{B}}$ per manganese atom was observed. These values are considerably lower than expected¹⁴ for six d^5 high-spin-configuration ions ($5.9 \mu_{\text{B}}$) and indicate the presence of antiferromagnetic interactions within the Mn_6N_4 cage. Such interactions have been observed in other manganese nitrogen species which contain short Mn...Mn distances.¹⁰

Acknowledgements

We are grateful to the donors of the Petroleum Research Fund administered by the American Chemical Society for financial support. We also thank David Randall for assistance with the collection of EPR data.

References

- 1 R. J. Debus, *Biochim. Biophys. Acta*, 1992, **1102**, 269 and refs. therein.
- 2 G. Christou, *Acc. Chem. Res.*, 1989, **22**, 328; D. P. Goldberg, A. Caneschi, C. D. Delfs, R. Sessoli and S. J. Lippard, *J. Am. Chem. Soc.*, 1995, **117**, 5789.
- 3 (a) A. A. Danopoulos, G. Wilkinson, T. Sweet and M. B. Hursthouse, *J. Chem. Soc., Chem. Commun.*, 1993, 495; (b) A. A. Danopoulos, G. Wilkinson, T. K. N. Sweet and M. B. Hursthouse, *J. Chem. Soc., Dalton Trans.*, 1994, 1037; (c) A. A. Danopoulos, G. Wilkinson, T. K. N. Sweet and M. B. Hursthouse, *J. Chem. Soc., Dalton Trans.*, 1995, 205; (d) A. A. Danopoulos, G. Wilkinson, T. K. N. Sweet and M. B. Hursthouse, *J. Chem. Soc., Dalton Trans.*, 1995, 937.
- 4 W. J. Grigsby, M. M. Olmstead and P. P. Power, *J. Organomet. Chem.*, 1996, **513**, 173; W. J. Grigsby, T. Hascall, J. J. Ellison, M. M. Olmstead and P. P. Power, *Inorg. Chem.*, 1996, **34**, 3254.
- 5 R. D. Shannon and C. T. Prewitt, *Acta Crystallogr., Sect. B*, 1969, **25**, 925.
- 6 SHELXTL, Version 5.02, A Program for Crystal Structure Determination, Siemens Analytical X-ray Instruments, Madison, WI, 1994.
- 7 XABS 2; an empirical absorption correction program, S. R. Parkin, B. Moezzi and H. Hope, *J. Appl. Crystallogr.*, 1995, **28**, 53.
- 8 W. A. Nugent and J. M. Mayer, *Metal-Ligand Multiple Bonds*, Wiley, New York, 1988.
- 9 T. Hascall, M. M. Olmstead and P. P. Power, *Angew. Chem., Int. Ed. Engl.*, 1994, **33**, 356.
- 10 H.-J. Mai, R. Meyer zu Köcker, S. Wocadlo, W. Massa and K. Dehnicke, *Angew. Chem., Int. Ed. Engl.*, 1995, **34**, 1235; H.-J. Mai, H.-C. Kang, S. Wocadlo, W. Massa and K. Dehnicke, *Z. Anorg. Allg. Chem.*, 1995, **621**, 1963; H.-J. Mai, B. Neumüller and K. Dehnicke, *Z. Naturforsch., Teil B*, 1996, **51**, 433.
- 11 C. E. Holloway and M. J. Melnik, *J. Organomet. Chem.*, 1994, **465**, 1.
- 12 L. Meunier, *C. R. Acad. Sci.*, 1903, **136**, 758.
- 13 W. Weltner, *Magnetic Atoms and Molecules*, Dover Publications, New York, 1983, pp. 266–277.
- 14 F. A. Cotton and G. Wilkinson, *Comprehensive Inorganic Chemistry*, Wiley, New York, 1988, p. 702.

Received 25th June 1996; Paper 6/04440I